Journal of Molecular Catalysis A: Chemical 379 (2013) 21–29

Contents lists available at ScienceDirect

Journal of Molecular Catalysis A: Chemical

journal homepage: www.elsevier.com/locate/molcata

Synthesis, characterization and catalytic application of some novel binuclear transition metal complexes of bis-(2-acetylthiophene) oxaloyldihydrazone for C—N bond formation

Divya Pratap Singh, Dushyant S. Raghuvanshi, K.N. Singh, Vinod P. Singh *

Department of Chemistry, Banaras Hindu University, Varanasi 221005, India

ARTICLE INFO

Article history:
Received 26 March 2013
Received in revised form 7 July 2013
Accepted 21 July 2013
Available online 30 July 2013

Keywords:
Binuclear metal complexes
Bis-(2-acetylthiophene) oxaloyldihydrazone
Single crystal X-ray diffraction study
Cyclovoltammetry
Catalytic activity

ABSTRACT

In the present work, synthesis, characterization and catalytic properties of some novel complexes derived from a Schiff base bis-(2-acetylthiophene) oxaloyldihydrazone with various transition metal ions and precursors have been reported. The complexes were characterized by IR, NMR, ESR, electronic and mass spectroscopy, magnetic moments and TGA studies. Molecular structures of the ligand and its Cu(I) complex are determined by single crystal X-ray diffraction. Electronic spectral studies exhibit a 6-coordinated geometry around metal centers for Co(II), Ni(II) and Cu(II) complexes, whereas 4-coordinated geometry for Cu(I) and Zn(II) complexes. ESR spectra indicate a distorted octahedral geometry for Cu(II) complex in DMSO frozen solution. The electro-chemical studies of Ni(II) and Cu(II) complexes reveal a metal based reversible redox behavior. The catalytic activity of the complexes has been demonstrated for the cross-coupling of arylboronic acids with various *N*-nucleophiles. Ni(II) complex exhibited the maximum impact on catalytic activity with the product yields ranging from 62% to 82%.

1. Introduction

The coordination chemistry of transition metal complexes of symmetrical dihydrazones has attracted considerable interest in recent years due to the formation of monometallic [1], homo-bimetallic [2] and hetrobimetallic [3] complexes with a variety of bonding and stereo-chemical possibilities [4,5]. The binuclear transition-metal complexes, particularly, have been widely used as catalysts in various organic reactions [6]. It has been observed that the binuclear Schiff base complexes of transition metal ions are more efficient catalysts than mononuclear complexes, probably due to the synergic effect of two metal ions [7]. The presence of two metal centers in close proximity in a complex has the potential of catalyzing reactions more effectively with different chemo-, regio- or stereo-selectivity than those of corresponding mononuclear ones, due to co-operation of the two metals in the transition state of the catalytic reaction [8,9]. The catalytic activities of a number of Schiff base complexes with transition metal(II) ions have been investigated [10–13].

The construction of C—N bond is an important key reaction with wide applications in the synthesis of organic functional molecules [14–18]. Despite the fundamental importance of C—N bond formation in organic synthesis, its construction remains often challenging and highly interesting in the development of new catalytic systems [19]. The Pd and Cu catalyzed coupling of electrophilic aryl halides and nucleophilic primary or secondary amines pioneered by Buchwald, Hartwig and others, are hallmark reactions in this field [20–24]. The groups of Chan, Evans and Lam (1998) have independently developed Cu-mediated oxidative amination of arylboronic acids with amines and other nucleophiles [25–28] and provided a valuable alternative to traditional cross-couplings in the construction of carbon-heteroatom bonds. Many extensions and applications of this new method have been reported, including the catalytic version of the reaction [29–32], arylation of amines under base and ligand-free conditions [33–36], tandem cross-coupling reactions [37] and solid-phase chemistry [38–42].

Although the reaction has been applied to a verity of substrates for carbon-hetero atom bond formation, but in all the cases copper salts have been repeatedly used in combination with different ligands, bases and solvents to promote the reaction [43,44]. To the best of our knowledge, no other metal has been reported in the literature to bring about the Chan–Lam reaction except a recent publication using nickel(II) chloride as catalyst [45]. Therefore, the catalytic role of newly synthesized transition metal complexes of thiophene ring containing Schiff bases has been investigated for the construction of C—N bond employing Chan–Lam strategies. Recently, some thiophene ring containing Schiff bases have been found to act as efficient catalyst for polymerization, hydrogenation, conjugate addition, Diels–Alder reactions and Henry reaction [46–49]. However, the use of such ligands in reactions catalyzed

* Corresponding author. Tel.: +91 9450145060.
E-mail address: singvp@yahoo.co.in (V.P. Singh).

1381-1169/$ – see front matter © 2013 Elsevier B.V. All rights reserved.
http://dx.doi.org/10.1016/j.molcata.2013.07.011

by transition metals is still relatively less explored as compared with other ligands. In view of the above, we report herein the synthesis and characterization of binuclear Co(II), Ni(II), Cu(II), Cu(I) and Zn(II) complexes derived from a symmetrical Schiff base bis-(2-acetylthiophene) oxaloyldihydrazone and investigate their subsequent applications in C—N cross-coupling of boronic acids and *N*-nucleophiles adopting Chan–Lam coupling.

2. Experimental

2.1. Materials and methods

All analytical reagent grade chemicals were obtained from the commercial sources and used without further purification. 2-Acetyl thiophene was purchased from Spectrochem Pvt. Ltd., India, oxalic acid dihydrazide from Sigma–Aldrich Chemicals, USA, metal(II) acetate and solvents from Merck Chemicals, India. The precursor bis-(triphenylphosphine) copper(I) nitrate was prepared by the reported procedure [50].

2.2. Synthesis of ligand

The ligand, bis-(2-acetylthiophene) oxaloyldihydrazone (H_2baoh) was synthesized by reacting 40 ml aqueous solution of oxalic acid dihydrazide (10 mmol, 1.18 g) with 20 ml methanolic solution of 2-acetylthiophene (20 mmol, 2.52 ml) in 1:2 molar ratio in a round bottom flask. A pale yellow solid product was obtained on refluxing the reaction mixture for 6 h and then cooling the solution at room temperature. The product was filtered on a Büchner funnel and purified by washing several times with water followed by methanol to remove the unreacted components. The pure compound was dried in a desiccator over anhydrous calcium chloride at room temperature. Single crystal of the ligand H_2baoh was obtained from a mixture of dichloromethane and DMSO solution by slow evaporation at room temperature. Yield (85%). M.p. 568 K. Anal. Calc. for $C_{14}H_{14}N_4O_2S_2$ (334): C, 50.28; H, 4.22; N, 16.75; S, 19.18. Found: C, 50.09; H, 4.20; N, 16.71; S, 19.14%. IR (ν cm^{-1}, KBr): ν(NH) 3259m; ν(CH$_3$) 2924w; ν(C=O) 1679s; ν(C=N) 1590m; ν(N—N) 990w. ^{1}H NMR (DMSO-d_6; δ ppm): 10.93 (s, 2H, NH); 7.63–7.62 (d, 2H, J = 4.5 Hz, thiophene moiety); 7.44–7.42 (d, 2H, J = 4.8 Hz, thiophene moiety); 6.98–6.96 (t, 1H, J = 8.1 Hz, thiophene moiety); 2.36 (s, 6H, CH$_3$). ^{13}C NMR (DMSO-d_6; δ ppm): 166.79 (C=O); 155.98 (C=N); 144.86 (C3); 142.12 (C6); 129.42 (C4); 127.91 (C5); 14.52 (CH$_3$).

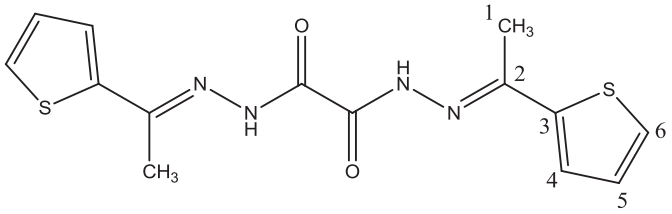

Bis-(acetylthiophene) oxaloyldihydrazone (H_2baoh)

2.3. Synthesis of the complexes

The Co(II), Ni(II), Cu(II) and Zn(II) complexes of bis-(2-acetylthiophene) oxaloyldihydrazone were synthesized by reacting 25 ml methanolic solutions of each metal(II) acetate (5 mmol) with 25 ml hot methanolic solution of the ligand H_2baoh (5 mmol, 1.67 g) separately, in 1:1 (M:L) molar ratio in a round bottom flask. The Co(II), Ni(II) and Zn(II) complexes were formed as insoluble precipitates after refluxing the reaction mixture for 2–5 h, whereas, Cu(II) complex was precipitated immediately on stirring the reaction mixture on a magnetic stirrer at room temperature. The metal complexes were filtered in a glass crucible and purified by washing several times with methanol and finally with diethyl ether. The complexes were dried in a desiccator at room temperature. The Cu(I) complex was synthesized by adding 25 ml methanolic solution of the ligand (1 mmol, 0.334 g) to a 25 ml solution of bis-(triphenylphosphine)copper(I) nitrate (2 mmol, 1.3 g) in dichloromethane in 2:1 (M:L) molar ratio. The reaction mixture was stirred on a magnetic stirrer for 24 h and the copper(I) complex was crystallized by slow evaporation of the solvent at room temperature.

2.3.1. [Co(baoh)(H$_2$O)$_2$]$_2$ (**1**)

Reddish brown, yield (70%). M.p. 547 K^d. μ_{eff} = 4.89 B.M. Anal. Calc. for $C_{28}H_{32}Co_2N_8O_8S_4$ (854.73): Co, 13.79; C, 39.35; H, 3.77; N, 13.11; S, 15.01. Found: Co, 13.80; C, 39.22; H, 3.79; N, 13.10; S, 14.95%. IR (ν cm^{-1}, KBr): ν(OH) 3408b; ν(CH$_3$) 2926w; ν(N=C—O$^-$) 1573m; ν(C=N) 1568m; ν(C—O)$^-$ 1244m; ν(N—N) 1022w.

2.3.2. [Ni(baoh)(H$_2$O)$_2$]$_2$·2H$_2$O (**2**)

Green, yield (80%). M.p. 485 K^d. μ_{eff} = 3.14 B.M. Anal. Calc. for $C_{28}H_{36}Ni_2N_8O_{10}S_4$ (890.28): Ni, 13.19; C, 37.77; H, 4.08; N, 12.59; S, 14.41. Found: Ni, 13.26; C, 37.65; H, 4.11; N, 12.65; S, 14.45%. IR (ν cm^{-1}, KBr): ν(OH) 3398s; ν(CH$_3$) 2929w; ν(N=C—O$^-$) 1571m; ν(C=N) 1566m; ν(C—O)$^-$ 1255m; ν(N—N) 1027w.

2.3.3. [Cu(baoh)(H$_2$O)$_2$]$_2$ (**3**)

Dirty green, yield (72%). M.p. 538 K^d. μ_{eff} = 1.83 B.M. Anal. Calc. for $C_{28}H_{36}Cu_2N_8O_8S_4$ (863.95): Cu, 14.71; C, 38.93; H, 3.73; N, 12.97; S, 14.85. Found: Cu, 14.67; C, 38.78; H, 3.75; N, 12.93; S, 14.81%. IR (ν cm^{-1}, KBr): ν(OH) 3439b; ν(CH$_3$) 2924w; ν(N=C—O$^-$) 1574m; ν(C=N) 1570m; ν(C—O)$^-$ 1245m; ν(N—N) 1022w.

2.3.4. [Cu$_2$(H$_2$baoh)(PPh$_3$)$_4$](NO$_3$)$_2$(CH$_2$Cl$_2$)$_2$ (**4**)

Yellow, yield (75%). M.p. 458 K. Anal. Calc. for $C_{88}H_{78}N_6O_8S_2Cu_2P_4Cl_4$ (1804.53): Cu, 7.04; C, 58.57; H, 4.36; N, 4.66; S, 3.55. Found: Cu, 7.01; C, 58.48; H, 4.39; N, 4.65; S, 3.53%. IR (ν cm^{-1}, KBr): ν(NH) 3263b; ν(CH$_3$) 2923w; ν(C=O) 1642s; ν(C=N) 1569m; ν(N—N) 1025w. ^{1}H NMR (DMSO-d_6; δ ppm): 11.25 (s, 2H, NH); 7.46–7.23 (m, phenyl and thiophene moieties); 2.42 (s, 6H, CH$_3$). ^{13}C NMR (DMSO-d_6; δ ppm): 167.14 (C=O); 158.91 (C=N); 143.23–127.37 (phenyl and thiophene moieties); 14.89 (CH$_3$). ^{31}P NMR (DMSO-d_6; δ ppm): 10.53 (s, 4P, PPh$_3$).

2.3.5. [Zn(baoh)]$_2$ (**5**)

Yellow, yield (68%). M.p. 558 K^d. Anal. Calc. for $C_{28}H_{24}Zn_2N_8O_4S_4$ (795.56): Zn, 16.44; C, 42.27; H, 3.04; N, 14.08; S, 16.12. Found: Zn, 16.35; C, 42.12; H, 3.05; N, 14.14; S, 16.20%. IR (ν cm^{-1}, KBr): ν(CH$_3$) 2927w; ν(N=C—O$^-$) 1577m; ν(C=N) 1572m; ν(C—O)$^-$ 1275; ν(N—N) 1021w. ^{1}H NMR (DMSO-d_6; δ ppm): 7.66–6.96 (m, thiophene moiety); 2.42 (s, 6H, CH$_3$). ^{13}C NMR (DMSO-d_6; δ ppm): 167.18 (N=C—O$^-$); 157.72 (C=N); 145.19–127.32 (thiophene moiety); 14.90 (CH$_3$).

2.4. Physico-chemical measurements

The molar conductance of 10^{-3} M solutions of the complexes in DMSO was measured at room temperature on a Eutech Con 510 Conductivity meter. ^{1}H, ^{13}C and ^{31}P NMR spectra of the ligand, complex **4** and complex **5** were recorded in DMSO-d_6 on a JEOL AL-300 FT-NMR multinuclear spectrometer. Chemical shifts were reported in parts per million (ppm) using tetramethylsilane (TMS) as an internal standard. All exchangeable protons were confirmed by addition of D_2O. Infrared spectra were recorded in KBr on a Varian 3100 FT-IR spectrophotometer in 4000–400 cm^{-1} region. Electronic spectra of the complexes were recorded on a Shimadzu

spectrophotometer model Pharmaspec UV-1700 in nujol. Magnetic susceptibility measurements were performed at room temperature on a Faraday balance using $Hg[Co(SCN)_4]$ as the calibrant and corrected for diamagnetism [51]. The ESR spectra of complex **3** in DMSO frozen solution at 77 K was recorded with a Varian E112 X-band spectrometer using 100 kHz field modulation. The *g* factors were quoted relative to the standard *g* marker TCNE ($g = 2.00277$). Electrochemical measurements were made with a bi-potentiostate CHI-660C (CH Instruments, USA). The thermograms (TGA) of the complexes **1**, **2** and **3** were recorded on a Perkin–Elmer STA 6000 Thermal analyzer, in the temperature range from room temperature to 900 °C at the rate of 10 °C min^{-1} in inert atmosphere.

2.5. Crystal structure determination

Single crystal X-ray diffraction data of the ligand and complex **4** were obtained at 295(2) K, on a Oxford Diffraction Gemini diffractometer equipped with CrysAlis Pro., using a graphite monochromated Mo Kα ($\lambda = 0.71073$ Å) radiation source. The structures were solved by direct methods (SHELXL-97) and refined against all data by full matrix least-square on F^2 using anisotropic displacement parameters for all non-hydrogen atoms. All hydrogen atoms were included in the refinement at geometrically ideal position and refined with a riding model [52,53]. The MERCURY package and ORTEP-3 for Windows program were used for generating structures [54,55].

2.6. General procedure for C—N cross-coupling

A 10 ml borosilicate vial containing arylboronic acid **I** (1 mmol), *N*-nucleophile **II** (2 mmol), complex (15 mol%), DBU (2 mmol) and acetonitrile (1 ml) was stirred at 40 °C. The progress of the reaction was monitored by TLC using ethyl acetate and *n*-hexane as eluent. After completion of reaction, the reaction mixture was filtered to remove the heterogeneous metal catalyst and the filtrate was treated with ethyl acetate (5 ml) and water (5 ml). The separated organic layer was washed twice with water (2 × 5 ml), dried over anhydrous sodium sulfate and concentrated to yield a residue. The residue was purified by silica gel column chromatography using hexane/ethyl acetate to yield clean product **III**.

3. Results and discussion

It appears from the analytical data that the reactions between Co(II), Ni(II), Cu(II) and Zn(II) acetates and ligand H_2baoh occur in 1:1 (M:L) molar ratio and the ligand enolizes and deprotonates during complexation. However, such enolization was not observed during the synthesis of Cu(I) complex by the reaction between ligand and bis-(triphenylphosphine) copper(I) nitrate in 2:1 (M:L) molar ratio. The reactions may be written as:

$$2H_2baoh + 2M(CH_3COO)_2{\cdot}xH_2O \rightarrow [M(baoh)(H_2O)_2]_2{\cdot}nH_2O + 4CH_3COOH$$

where M = Co(II), Ni(II) and Cu(II); $n = 0$ for Co(II) and Cu(II); $n = 2$ for Ni(II)

$$2H_2baoh + 2Zn(CH_3COO)_2{\cdot}xH_2O \rightarrow [Zn(baoh)]_2 + 4CH_3COO + xH_2O$$

$$H_2baoh + 2(PPh_3)_2Cu(NO_3) \rightarrow [Cu_2(H_2baoh)(PPh_3)_4](NO_3)_2(CH_2Cl_2)_2$$

The metal complexes are colored powdery solids. The complexes **1**, **2**, **3**, and **5** are insoluble in water and most of the organic solvents like ethanol, methanol, chloroform, benzene and diethyl ether but are soluble in DMF and DMSO. The complex **4** is also soluble in water, dichloromethane and chloroform. The complexes melt with decomposition in the temperature range 485–558 K. 10^{-3} M solutions of the complexes **1**, **2**, **3** and **5** in DMSO show low molar conductance values (3.46–8.08 Ω^{-1} mol^{-1} cm^2) at room temperature, indicating that they are non-electrolytes [56]. However, the complex **4** is 1:1 electrolyte with a molar conductance value 58.18 Ω^{-1} mol^{-1} cm^2.

3.1. IR spectra

The IR spectral bands observed at 3259, 1679, 1590 and 992 cm^{-1} in the free ligand are assigned to ν(N—H), ν(C=O), ν(C=N) and ν(N—N), respectively [57]. The ν(C=O) and ν(N—H) bands are absent in the complexes **1**, **2**, **3** and **5** due to the enolization of both carbonyl groups of the ligand during complex formation [58]. The appearance of a new $\nu(C{-}O)^-$ band in these complexes in the range 1244–1275 cm^{-1} suggests bonding of the ligand through two deprotonated $C{-}O^-$ groups to metal [59]. In all the metal complexes, the band due to ν(C=N) has been shifted to lower frequency (18–24 cm^{-1}) as compared to free ligand, suggesting the participation of both azomethine nitrogen in coordination [60]. The complexes **1**, **2**, **3** and **5** also show an additional ν(C=N) band in the range 1571–1577 cm^{-1} due to creation of two new >C=N— groups as a result of enolization. The presence of ν(N—H) in complex **4** at 3263 cm^{-1} and ν(C=O) at lower wave number (37 cm^{-1}) indicates the coordination of both >C=O groups to metal and non-participation of N—H group in bonding. Furthermore, the ν(N—N) has been shifted to higher frequency (31–37 cm^{-1}) in all the complexes as compared to the free ligand, indicating the involvement of one of the nitrogen atoms of >N—N< moiety in bonding. The complexes **1**, **2** and **3** show a broad band centered in the range 3398–3439 cm^{-1} due to ν(OH) of water molecules. The weak bands observed in the ranges 949–954, 779–784 and 650–664 cm^{-1} in these complexes also suggest the presence of coordinated water molecules [60]. The bands due to ν(C—S—C) of the thiophene ring of ligand observed in the range 828–845 cm^{-1}, keep their positions in the metal complexes indicating non-involvement of the thiophene-S in bonding.

3.2. ^1H, ^{13}C and ^{31}P NMR spectra

The ^1H NMR spectrum of H_2baoh in DMSO exhibits a signal at 10.93 ppm for —NH proton, confirming existence of the ligand in keto form (Fig. S1). The disappearance of —NH proton signal in the complex **5** indicates that both —NH groups of the ligand deprotonate during complex formation. However, the —NH proton signal appears at 11.25 ppm in the complex **4**. The ^1H NMR signals for the thiophene ring protons are observed at 7.63–7.62 ppm as a doublet, 7.44–7.42 ppm as a doublet and 6.98–6.96 ppm as a triplet in ligand. These signals are observed as multiplet in the complex **5** in the range 7.66–6.96 ppm (Fig. S2). In the complex **4**, the thiophene and phenyl protons appear as multiplets in the range 7.46–7.23 ppm (Fig. S3). The ligand shows a sharp singlet at 2.36 ppm due to the methyl ($-CH_3$) protons which undergoes a downfield shift and appears at 2.42 and 2.42 ppm, respectively in the complexes **4** and **5**, due to coordination of the azomethine nitrogen [61,62].

The number of carbon signals in ^{13}C NMR spectra of the ligand as well as in its complexes **4** and **5** corresponds well to the number of carbon atoms present in these molecules. The ^{13}C NMR spectrum of the ligand exhibits a cluster of peaks between 144.86 and 127.91 ppm corresponding to aromatic carbons of the thiophene rings (Fig. S4). The signals at 14.52, 155.98 and 166.79 ppm in the ligand are assigned to $-CH_3$, >C=N— and >C=O carbons. A low field signal due to >C=N— observed at 157.72 ppm and appearance of a

new signal due to —N=C—O⁻ carbons at 167.18 ppm in the complex **5** indicate bonding of C=N and C—O⁻ groups with metal (Fig. S5). The ^{13}C NMR spectrum of the complex **4** shows multiplet peaks between 143.23 and 127.37 ppm corresponding to aromatic carbons of the thiophene and phenyl rings. The signals due to —CH_3, >C=N— and >C=O carbons show low field shift in the complex **4** and appear at 14.89, 158.91 and 167.14 ppm, respectively, indicating the bonding of >C=N— and >C=O groups with metal (Fig. S6). The ^{31}P NMR spectra of the complex **4** show a peak at 10.53 ppm due to PPh_3.

3.3. Electronic spectra and magnetic moments

Cobalt(II) complexes generally show three d–d electronic transitions in the visible range, $^4T_{1g}(F) \rightarrow {}^4T_{2g}(F)$, $^4T_{1g}(F) \rightarrow {}^4A_{2g}(F)$ and $^4T_{1g}(F) \rightarrow {}^4T_{1g}(P)$ in an octahedral field. In the present study, the complex **1** exhibits three bands at 9311, 17,241 and 24,631 cm^{-1}, respectively, suggesting an octahedral geometry for the complex [63]. The complex **1** shows μ_{eff} value, 4.89 B.M., corresponding to three unpaired electrons with an octahedral geometry [51]. The d–d transition spectra of complex **2** shows three bands at 11,507, 16,393 and 24,752 cm^{-1}, which may be assigned to $^3A_{2g}(F) \rightarrow {}^3T_{1g}(F)$, $^3A_{2g}(F) \rightarrow {}^3T_{2g}(F)$ and $^3A_{2g}(F) \rightarrow {}^3T_{1g}(P)$ transitions, respectively, in an octahedral environment around metal ion [64]. The μ_{eff} value, 3.14 B.M. obtained for the complex **2** is in good agreement with a high spin octahedral species, establishing the triplet ground state. The complex **3** exhibits three d–d electronic spectral bands at 15,773, 23,202 and 24,155 cm^{-1}, which may be assigned to $^2B_{1g} \rightarrow {}^2A_{1g}$, $^2B_{1g} \rightarrow {}^2B_{2g}$ and $^2B_{1g} \rightarrow {}^2E_g$, indicating a distorted octahedral geometry for the complex [63]. This complex shows μ_{eff} value 1.83 B.M. corresponding to one unpaired electron.

3.4. ESR spectra

ESR spectra of complex **3** in DMSO frozen solution at 77 K give axial signal with a well resolved hyperfine structure of four lines due to copper(II) nuclei ($I = 3/2$) on the low field region to allow accurate calculation of $g_{||}$ and $A_{||}$ values (Fig. S7). The calculated g and A values are, $g_{||} = 2.428$, $g_{\perp} = 2.093$, $A_{||} = 176$ and $A_{\perp} = 70$. These values predict a distorted octahedral geometry for the complex. Moreover, the trend $g_{||} > g_{\perp} > g_e$ (2.0023), suggests that the ground state of copper(II) is predominantly $d_{x^2-y^2}$ [65,66]. The presence of an intense half-field signal at 1540 G, due to $\Delta Ms = 2$ transition in the complex, strongly suggests the dimeric nature of the complex [67].

3.5. Mass spectra

The mass spectrum of the complex **1** exhibits a base peak at $m/z = 521.1$, corresponding to a fragment of the complex produced on removing the thiophene moieties of the ligands. The molecular ion peak with highest m/z value, indicating the molecular weight of the complex **1**, has been observed at $m/z = 855.6$ with 15% intensity (Fig. S8). A peak observed at $m/z = 334.9$, corresponds to ligand.

The complex **2** shows molecular ion peak at $m/z = 890.5$ with 45% intensity (Fig. S9). The base peak observed at $m/z = 722.8$ in the mass spectrum of the complex, corresponds well with a complex fragment without water and methyl groups of the bonded ligands. A peak with $m/z = 334.9$ corresponding to the ligand has also been observed.

On the basis of above spectral studies, general structures for the metal complexes have been proposed in Fig. 1.

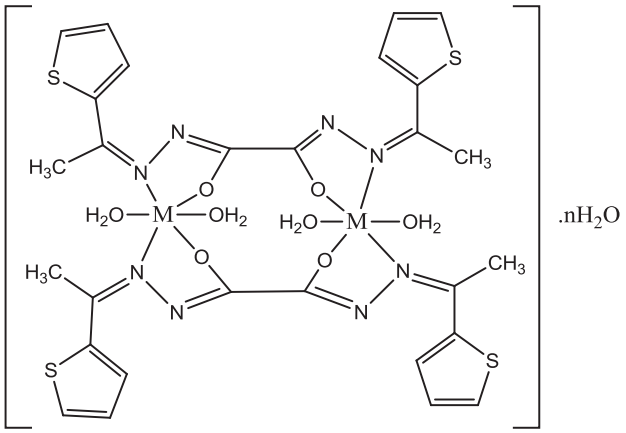

M = Co(II), Ni(II) and Cu(II)

n = 0 for **1** and **3**; n = 2 for **2**

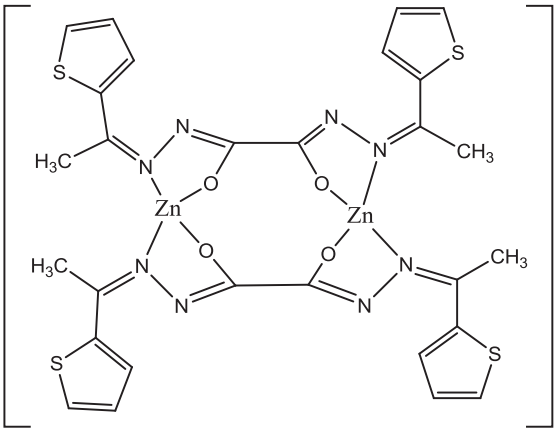

Fig. 1. Representative structures of the complexes.

3.6. Thermal decomposition study (TGA)

The complex **1** shows multi-step decomposition pattern in TGA analysis (Fig. S10). It loses weight between 120 and 205 °C corresponding to four water molecules. The removal of water molecules at high temperature indicates that they are coordinated water. The removal of four CH_3 and four thiophene moieties of the ligand molecules occur in the temperature ranges 205–310 and 310–420 °C, respectively. The complex further loses weight in the temperature range 420–615 °C due to removal of four —C=N—N=C— moieties and changes to Co_2O_4. Finally, the complex loses two oxygen atoms in the range 615–900 °C to form CoO as the stable end product.

TGA curve of complex **2** shows weight loss between room temperature to 105 °C corresponding to two lattice water molecules (Fig. S11). Further, it loses weight between 105 and 180 °C due to the removal of four coordinated water molecules. The removal of four CH_3 along with four thiophene moieties of the bonded ligand molecules occurs in the temperature range 180–405 °C. The complex further undergoes decomposition and loses weight in the temperature range 405–580 °C due to removal of four —C=N—N=C— moieties. Finally, the complex removes two oxygen atoms in the range 580–900 °C to form NiO at 900 °C.

The complex **3** is stable up to 120 °C and then loses weight between 120 and 200 °C corresponding to four coordinated water

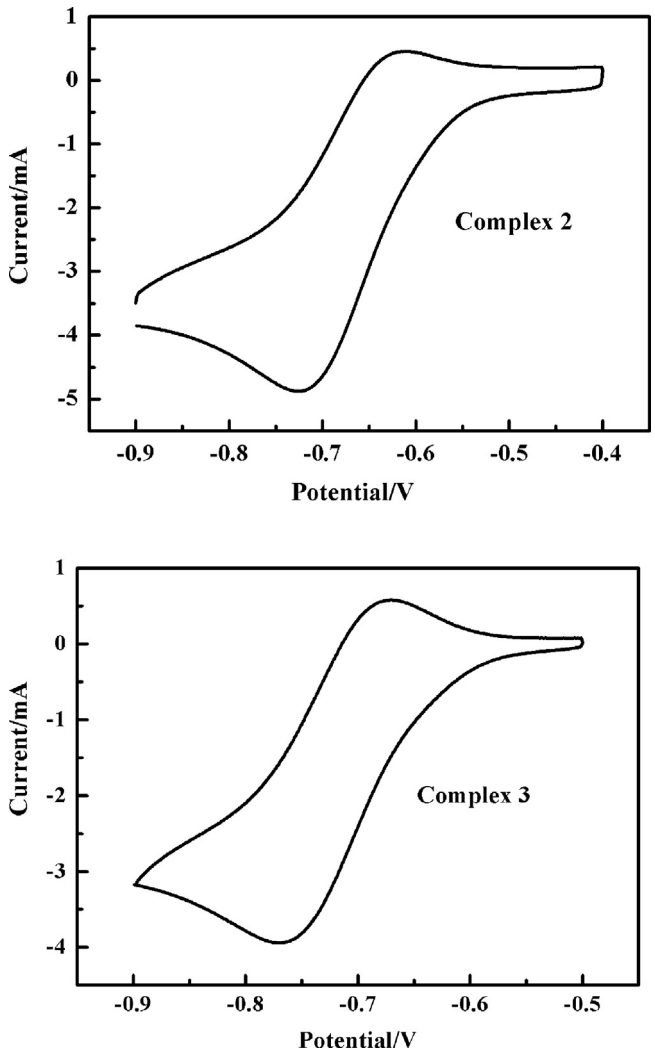

Fig. 2. Cyclic voltammograms of the complexes **2** and **3**.

molecules. An appreciable change in weight of the complex occurs due to decomposition of four CH_3 and four thiophene moieties of the bonded ligands together in the temperature range 200–310 °C. TGA curve of the complex **3** shows that the decomposition process is still incomplete up to 900 °C and removal of the remaining parts of bonded ligand continues (Fig. S12). The proposed decomposition schemes for the complexes have been given in Table S1.

3.7. Cyclic voltammetry

The redox potential is an important parameter as it characterizes the ability of the redox center to transfer electrons and also to act as a redox catalyst. In metal complexes, the redox behavior of metal center is also influenced by the nature of the bonded ligands to the metal. The electrochemical behavior of the present ligand and its complexes **2** and **3** were examined by employing glassy carbon as working electrode, Ag/AgCl as reference electrode and platinum wire as auxiliary electrode. The working media consisted of DMSO and tetra(*n*-butyl) ammonium perchlorate (TBAP) as supporting electrolyte. The cyclic voltammogram of the ligand and its complexes **2** and **3** were recorded at room temperature in the potential range −0.9 to −0.4 with a scan rate 50 mV s^{-1}.

The complexes **2** and **3** show redox peaks in the applied potential range where, the ligand does not show electrochemical response, revealing that the redox behavior exhibited by the complexes **2** and **3** are purely metal based. The cyclic voltammogram of complex **2** shows an anodic peak at the potential E_{pa} = −0.617 V and a cathodic peak at the potential E_{pc} = −0.725 V (Fig. 2). The half wave potential $E_{1/2}$ = −0.671 V, the difference between the peak ΔE_p = 0.108 V and peak current ratio I_{pa}/I_{pc} = 0.9, suggests that it is a one electron quasi reversible process.

The cyclic voltammogram of complex **3** exhibits an anodic peak at the potential E_{pa} = −0.670 V and a cathodic peak at the potential E_{pc} = −0.768 V. These redox peaks can be attributed to $Cu^{2+} + e^- \rightleftharpoons Cu^+$, exhibiting a reversible process [68]. The half wave potential located at $E_{1/2}$ = −0.719 V, the difference between the peaks ΔE_p = 0.098 V, and peak current ratio I_{pa}/I_{pc} = 1.4 indicate one electron quasi reversible process also for the complex **3**.

Table 1
Crystallographic data for H_2baoh and complex **4**.

	H_2baoh	Complex **4**
Empirical formula	$C_{14}H_{14}N_4O_2S_2$	$C_{88}H_{74}N_6O_8S_2Cu_2P_4Cl_4$
Formula weight	334.41	1804.48
Temperature (K)	293(2)	293(2)
λ (Å)	0.71073	0.71073
Crystal system	Monoclinic	Monoclinic
Space group	*C*2/*c*	*P*21/*n*
a (Å)	35.892(5)	13.8604(14)
b (Å)	5.189(5)	22.608(3)
c (Å)	8.459(5)	13.8990(18)
α (°)	90	90
β (°)	99.864(5)	99.221(9)
γ (°)	90	90
V (Å^3)	1552.1(18)	4299.1(9)
Z	4	2
D_{calc} (g/cm^3)	1.431	1.394
μ (mm^{-1})	0.355	0.801
F(0 0 0)	696.0	1860.0
Crystal size (mm)	0.32 × 0.30 × 0.28	0.34 × 0.32 × 0.30
θ range for data collection (°)	3.46–29.09	3.10–28.93
No. of reflections collected	2083	11,347
No. of independent reflections (R_{int})	2083 (0.0502)	11,347 (0.0398)
Number of data/restraints/parameters	2083/1/104	11,347/15/504
Goodness-of-fit on F^2	1.060	1.065
R_1, wR_2 [a,b] [($I > 2\sigma(I)$)]	0.0668, 0.1801	0.0774, 0.2039
R_1, wR_2 [a,b] (all data)	0.1107, 0.2280	0.1259, 0.2547
Largest difference in peak and hole (e Å^{-3})	0.363 and −0.462	0.989 and −0.561

[a] $R_1 = \Sigma||F_o| - |F_c||\Sigma|F_o|$.

[b] $R_2 = \left[\frac{\sum w(|F_o^2| - |F_o^2|)^2}{\sum w|F_o^2|^2}\right]^{1/2}$.

3.7.1. Single crystal structure of the ligand

The crystallographic data, structural refinement details, selected bond lengths and bond angles of free ligand and the complex **4** are given in Tables 1–3, respectively. Fig. 3 shows the ORTEP diagram of the ligand with atomic numbering scheme. The molecular structure of the ligand stabilizes by intra-molecular N—H···O (2.052 Å) and intermolecular C—H···N (2.705 Å) weak

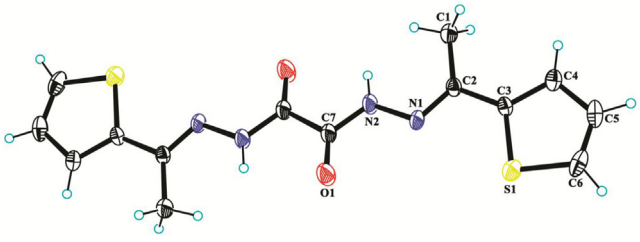

Fig. 3. ORTEP diagram of ligand showing atomic numbering scheme with ellipsoid of 30% probability.

Table 2
Selected bond lengths (Å) and angles (°).

	H_2baoh	Complex **4**
Bond length		
C(2)—N(1)	1.279(4)	1.292(7)
C(7)—O(1)	1.200(5)	1.222(6)
N(2)—C(7)	1.346(5)	1.336(7)
N(1)—N(2)	1.370(4)	1.399(5)
C(1)—C(2)	1.481(5)	1.496(8)
N(1)—Cu(1)		2.131(4)
O(1)—Cu(1)		2.233(3)
P(1)—Cu(1)		2.281(16)
P(2)—Cu(1)		2.244(15)
Bond angle		
O(1)—C(7)—N(2)	126.4(3)	124.8(5)
C(7)—N(2)—N(1)	119.6(3)	116.2(4)
Cu(1)—N(1)—N(2)		111.5(3)
Cu(1)—O(1)—C(7)		109.7(3)
N(1)—Cu(1)—O(1)		75.42(14)
P(1)—Cu(1)—P(2)		123.07(5)
O(1)—Cu(1)—P(1)		93.96(11)
O(1)—Cu(1)—P(2)		114.78(11)
N(1)—Cu(1)—P(1)		114.14(12)
N(1)—Cu(1)—P(2)		120.02(13)

Table 3
Hydrogen bond parameters [Å and°] in the complex **4**.

D—H···A	D—H	H···A	D···A	⟨(DHA)
N(2)—H(2)···O(4)	0.86	2.147	2.917	148.82

1/2 − *x*, 1/2 + *y*, 3/2 − *z*.

interactions forming a supra-molecular architecture on axis '*c*' (Fig. 4). The molecule displays an *E* configuration about the C=N bond [69]. The C(7)—O(1) and C(2)—N(1) display bond distances of 1.200(5) and 1.279(4) Å, respectively as reported for double bonds [70]. All the C—C bond lengths (1.378 Å) and C—C—C bond angles (112.22°) of the thiophene ring as well as the C—S bond length (1.695 Å) and C—S—C angle (91.8°) are in accordance with a typical thiophene moiety [71]. The torsion angles S(1)—C(3)—C(2)—N(2) [1.01], N(2)—N(1)—C(2)—C(3) [−176.7°], N(2)—N(1)—C(2)—C(1) [−2.7] and S(1)—C(3)—C(2)—C(1) [−178.4°] indicate that N(2)—O(1) and S(1)—N(1) are *cis* to each other but S(1)—C(1) are *trans* to each other [72].

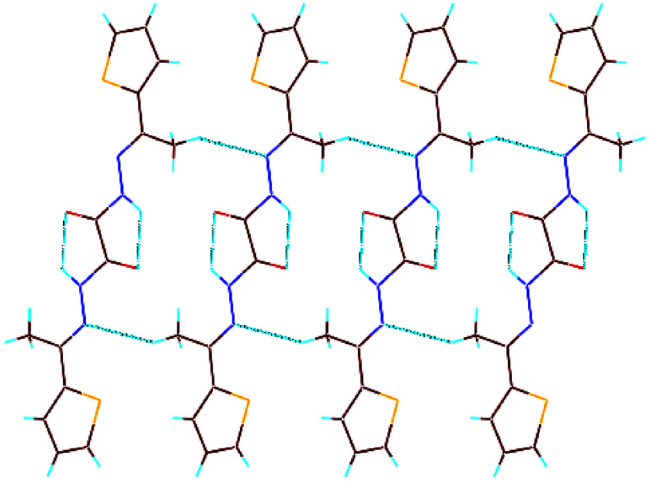

Fig. 4. Diagram showing intra-molecular N—H···O and intermolecular C—H···N interactions in the ligand, forming supra-molecular structure along *c*-axis.

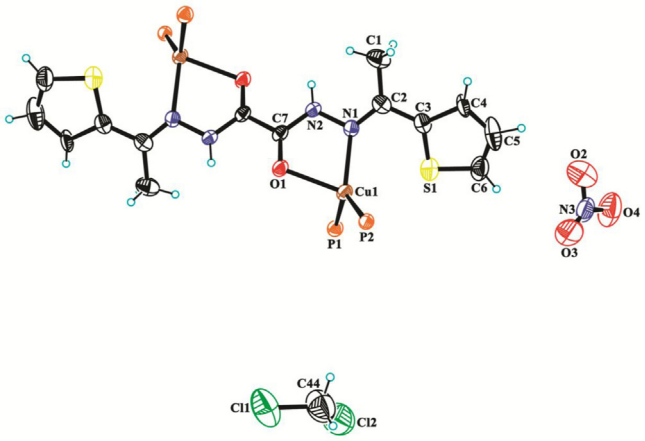

Fig. 5. ORTEP diagram of the complex **4** showing atomic numbering scheme with ellipsoid of 30% probability (phenyl rings are omitted for clarity).

3.7.2. *Single crystal structure of complex* ***4***

Fig. 5 shows the ORTEP diagram of the complex **4** with atomic numbering scheme. Packing diagram of the complex **4** on *a*-axis, showing intermolecular H-bonding, is shown in Fig. 6. In the binuclear complex **4**, each metal center is coordinated with NOP_2 core by using azomethine nitrogen and a carbonyl oxygen atom of H_2baoh ligand, and two phosphorous atoms of triphenylphosphine ligands. The two metal ions in the complex are arranged in a *trans* manner to the coordinating sites of ligands. The average bond lengths in the complex are: C(7)—N(2) = 1.336(7), C(7)—O(1) = 1.222(6) and N(1)—N(2) = 1.399(5) Å, respectively which are longer or shorter than those of the corresponding distances in the ligand. The Cu—O(1) and Cu—N(1) bond distances are 2.233(3) and 2.131(4) Å, which fall in the range reported for Cu(I) tetrahedral complexes [73]. The C(2)—N(1) distance (1.292 Å) in the complex is significantly longer than the free ligand (1.279 Å) due to coordination of azomethine nitrogen to the metal ion. Similarly, the C(7)—O(1) distance (1.222 Å) in the complex is longer than the ligand (1.200 Å) as a result of involvement of O atom in bonding. The torsion angle of 169.2(5)° exhibited by S(1)—C(3)—C(2)—C(1) indicates that the C(1) of methyl group is in *trans* position to the sulfur of thiophene moiety. The torsion angles S(1)—C(3)—C(2)—N(1) [−12.0°],

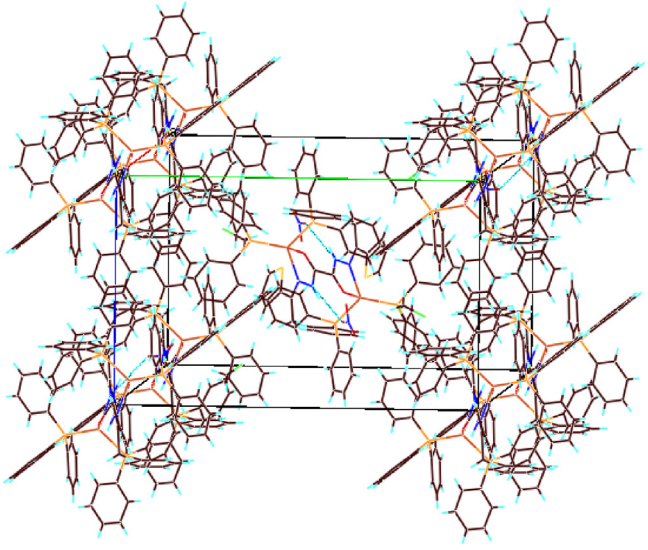

Fig. 6. Packing diagram of the complex **4** showing intermolecular H-bonding on *a*-axis.

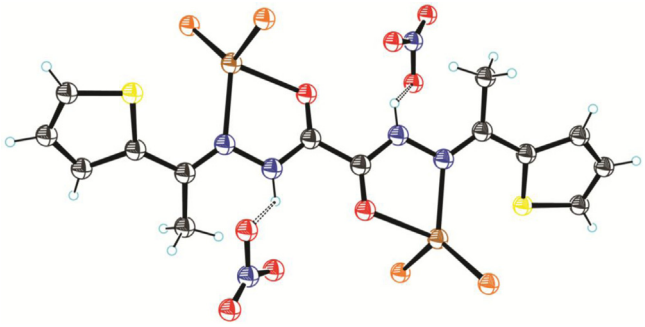

Fig. 7. Diagram showing intermolecular hydrogen bonding in the complex **4**. Hydrogen bonds are shown by dashed lines (phenyl rings are omitted for clarity).

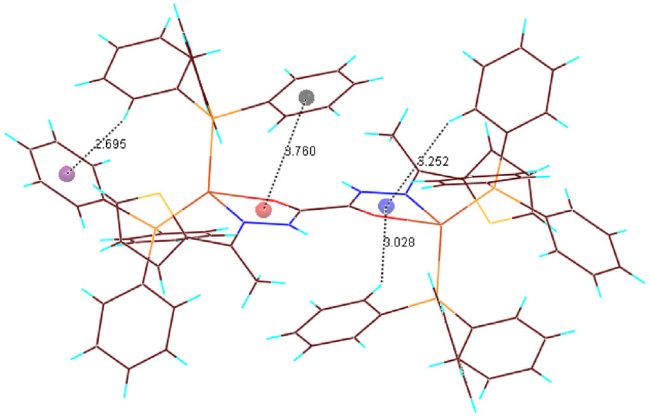

Fig. 8. Diagram showing intra-molecular π–π stacking and C—H···π interactions along '*c*' axis in the complex **4**.

N(2)—N(1)—C(2)—C(3) [168.7°] and N(2)—N(1)—C(2)—C(1) [−13.3°] indicate that N(2)—O(1) and S(1)—N(1) are *cis* to each other but S(1)—C(1) are *trans* to each other [72].

The molecular structure of the complex is stabilized by intermolecular N(2)—H(2)···O(4) hydrogen bonding and intra-molecular edge to face π–π and C—H···π interactions (Figs. 7 and 8). Edge to face π–π stacking occurs between the centroid of the chelate ring and phenyl ring with a contact distance of 3.760 Å [74], while the C—H···π interaction occurs between a phenyl proton and the centroid of the phenyl ring with a contact distance of 2.695 Å. The C—H···π interactions also take place when phenyl protons approach the centroid of the chelate rings with contact distances of 3.028 and 3.252 Å [75].

3.8. Catalytic properties

The catalytic efficiency of the newly synthesized complexes **1**–**5** was explored for the C—N bond formation involving the Chan–Lam coupling. In order to optimize the reaction conditions, a typical reaction of phenylboronic acid and aniline was carried out in acetonitrile by varying different parameters. The outcome is given in Table 4. The findings reveal that out of all the complexes used, the complex **2** (15 mol%) at 40 °C affords the maximum yield (80%) of the product **IIIa** (Table 4, entry 5). A further increase in the catalyst loading and temperature could not enhance the product yield again (Table 4, entries 6–8). The use of other complexes **3** and **4** as catalyst also promoted the reaction to a reasonable extent (Table 4, entries 9 and 10), but the complexes **1** and **5** did not afford any conversion (Table 4, entries 3 and 11). A control experiment using $NiCl_2{\cdot}6H_2O$ (15 mol%), without the aid of a ligand, afforded only 18% product yield. The experiment under identical conditions, without the aid of a nickel complex, ended with no conversion. Thus, the complex **2** (15 mol%) with DBU (2 equiv.) in acetonitrile at 40 °C, was finally concluded to be the optimum condition for further studies. Under the stipulated conditions, we explored the scope and feasibility of the aforementioned reaction by using phenylboronic and *p*-tolylboronic acids **I** with different aromatic amines **II**, and the outcome is given in Table 5. It is interesting to observe that different aniline derivatives containing electron donating/withdrawing group and morpholine undergo reactions smoothly in the presence of complex **2** and produce the corresponding *N*-arylated products in 62–82% yields. The physical and spectral data of all the products are in full agreement with their assigned structures (Figs. S13–S30).

Table 4
Optimization of the reaction conditions.[a]

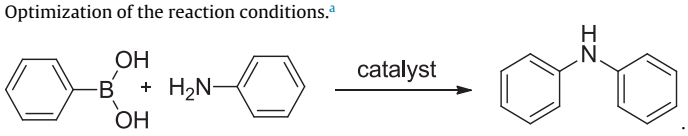

Entry	Catalyst	Base	Temperature (°C)	Solvent	Yield[b] (%)
1	–	DBU	40	CH_3CN	nr[c]
2	$NiCl_2{\cdot}6H_2O$ (15 mol%)	DBU	40	CH_3CN	18
3	Complex **1** (15 mol%)	DBU	40	CH_3CN	nr[c]
4	Complex **2** (10 mol%)	DBU	40	CH_3CN	68[d]
5	Complex **2** (15 mol%)	DBU	**40**	CH_3CN	**80**
6	Complex **2** (20 mol%)	DBU	40	CH_3CN	80[e]
7	Complex **2** (15 mol%)	DBU	RT	CH_3CN	55
8	Complex **2** (15 mol%)	DBU	60	CH_3CN	80
9	Complex **3** (15 mol%)	DBU	40	CH_3CN	40
10	Complex **4** (15 mol%)	DBU	40	CH_3CN	55
11	Complex **5** (15 mol%)	DBU	40	CH_3CN	nr[c]

The bold values signify the best optimised reaction conditions and product yield.

[a] *Reaction conditions*: Phenyllboronic acid (1 mmol), aniline (2 mmol), catalyst (15 mol%), CH_3CN (1 ml), 40 °C, 15 h.
[b] Isolated yield based on arylboronic acid.
[c] No reaction.
[d] Catalyst (10 mol%).
[e] Catalyst (20 mol%).

Table 5
Coupling of arylboronic acid with a range of *N*-nucleophiles.[a]

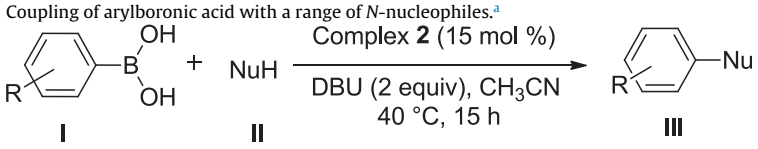

I II III

Entry	I	II	III	Yield[b] (%)
1	H	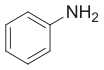	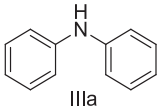 IIIa	80
2	H	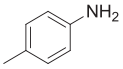	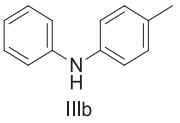 IIIb	82
3	H	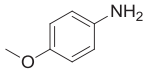	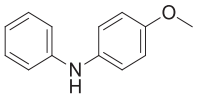 IIIc	78
4	H	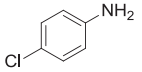	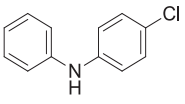 IIId	76
5	H	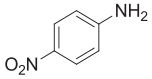	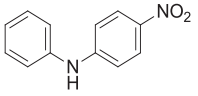 IIIe	67
6	H	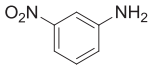	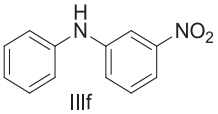 IIIf	62
7	H		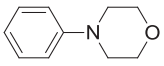 IIIg	70
8	4-Me	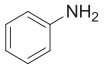	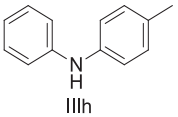 IIIh	75
9	4-Me	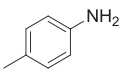	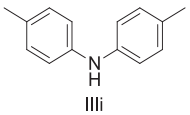 IIIi	76
10	4-Me	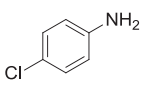	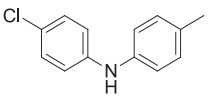 IIIj	81

[a] *Reaction conditions*: Arylboronic acid (1 mmol), *N*-nucleophile (2 mmol), complex **2** (15 mol%), CH_3CN (1 ml), 40 °C, 15 h.
[b] Isolated yield based on arylboronic acid.

4. Conclusions

The present work describes the synthesis of a symmetrical Schiff base ligand bis-(2-acetylthiophene) oxaloyldihydrazone (H_2baoh), and its binuclear metal complexes **1**, **2**, **3**, **4** and **5**. These were characterized by various spectroscopic techniques. The molecular structures of the ligand and its complex **4** have also been determined by X-ray crystallography. The complex **4** stabilizes by

intermolecular hydrogen bonding and intra-molecular edge to face π–π and C—H···π interactions. The catalytic efficiency of the newly synthesized complexes has been demonstrated for the C—N bond formation using Chan–Lam coupling. The complex **2** has been found to exhibit maximum impact on catalytic activity at 40 °C in acetonitrile.

Supplementary material

CCDC 911667 and 898068 contain the supporting information crystallographic data for the ligand H2baoh and complex **4**, respectively. These data can be obtained free of charge via http://www.ccdc.cam.ac.uk/conts/retrieving.html, or from the Cambridge Crystallographic Data Centre, 12 Union Road, Cambridge CB2 1EZ, UK; fax: (+44) 1223-336-033; or e-mail: deposit@ccdc.cam.ac.uk. The characterization data of the ligand and products are given in supporting information.

Acknowledgements

The authors thank the Head, S.A.I.F., Indian Institute of Technology, Mumbai and Central Drug Research Institute, Lucknow for recording the ESR and mass spectra, respectively. One of the authors (D.P.S.) is also grateful to CSIR, New Delhi for financial assistance in the form of Senior Research Fellowship.

Appendix A. Supplementary data

Supplementary material related to this article can be found, in the online version, at http://dx.doi.org/10.1016/j.molcata.2013.07.011.

References

[1] V. Niel, V.A. Milway, L.N. Dawe, H. Grove, S.S. Tandon, T.S.M. Abedin, T.L. Kelly, E.C. Spencer, J.A.K. Howard, J.L. Collins, D.O. Miller, L.K. Thompson, Inorg. Chem. 47 (2008) 176–189.
[2] V.P. Singh, S. Singh, J. Coord. Chem. 64 (2011) 3068–3080.
[3] A. Kumar, R. Borthakur, A. Koch, O.B. Chanu, S. Choudhury, A. Lemtur, R.A. Lal, J. Mol. Struct. 999 (2011) 89–97.
[4] A.M. Stadler, J. Harrowfield, Inorg. Chim. Acta 362 (2009) 4298–4314.
[5] G.G. Mohamed, M.M. Omar, Ahmed M.M. Hindy, Spectrochim. Acta Part A 6 (2005) 1140–1150.
[6] A.G.J. Ligtenbarg, E.K. van den Beuken, A. Meetsma, N. Veldman, W.J.J. Smeets, A.L. Spe, B.L. Feringa, J. Chem. Soc. Dalton Trans. (1998) 263–270.
[7] K.C. Gupta, A.K. Sutar, Coord. Chem. Rev. 252 (2008) 1420–1450.
[8] H. Steinhagen, G. Helmchen, Angew. Chem. Int. Ed. Engl. 35 (1996) 2339–2342.
[9] W.J. Peng, S.G. Train, D.K. Howell, F.R. Fronczek, G.G. Stanley, Chem. Commun. (1996) 2607–2612.
[10] Z. Chen, H. Morimoto, S. Matsunaga, M. Shibasaki, J. Am. Chem. Soc. 130 (2008) 2170–2171.
[11] Y.N. Belokon, N.B. Bespalova, T.D. Churkina, I. Císařová, M.G. Ezernitskaya, S.R. Harutyunyan, R. Hrdina, H.B. Kagan, P. Kočovský, K.A. Kochetkov, O.V. Larionov, K.A. Lyssenko, M. North, M. Polášekr, A.S. Peregudov, V.V. Prisyazhnyuk, S. Vyskočil, J. Am. Chem. Soc. 125 (2003) 12860–12864.
[12] S. Handa, V. Gnanadesikan, S. Matsunaga, M. Shibasaki, J. Am. Chem. Soc. 129 (2007) 4900–4901.
[13] D. Sadhukhan, A. Ray, G. Pilet, C. Rizzolis, G.M. Rosair, C.J. Gomez-Garcia, S. Signorella, S. Bellu, S. Mitra, Inorg. Chem. 50 (2011) 8326–8339.
[14] J.F. Hartwig, Nature 455 (2008) 314–322.
[15] H.Y. Lee, J.Y. Chang, L.Y. Chang, W.Y. Lai, M.J. Lai, K.H. Shih, C.C. Kuo, C.Y. Chang, J.P. Liou, Org. Biomol. Chem 9 (2011) 3154–3157.
[16] C. Fischer, B. Koenig, Beilstein J. Org. Chem 7 (2011) 59–74.
[17] S. Ueda, M. Su, S.L. Buchwald, J. Am. Chem. Soc. 134 (2012) 700–706.
[18] R. Hili, A.K. Yudin, Nat. Chem. Biol. 2 (2006) 284–287.
[19] T.E. Müller, M. Grosche, E. Herdtweck, A.K. Pleier, E. Walter, Y.K. Yan, Organometallics 19 (2000) 170–183.
[20] J. Louie, J.F. Hartwig, Tetrahedron Lett. 36 (1995) 3609–3612.
[21] A.S. Guram, R.A. Rennels, S.L. Buchwald, Angew. Chem. Int. Ed. Engl. 34 (1995) 1348–1350.
[22] D. Ma, Y. Zhang, J. Yao, S. Wu, F. Tao, J. Am. Chem. Soc. 120 (1998) 12459–12467.
[23] H.B. Goodbrand, N.X. Hu, J. Org. Chem. 64 (1999) 670–674.
[24] A. Klapars, J.C. Antilla, X. Huang, S.L. Buchwald, J. Am. Chem. Soc. 123 (2001) 7727–7729.
[25] D.M.T. Chan, K.L. Monaco, R.P. Wang, M.P. Winters, Tetrahedron Lett. 39 (1998) 2933–2936.
[26] J.J. Li, Name Reaction, fourth ed., Springer, Berlin, 2009, pp. 101.
[27] P.Y.S. Lam, C.G. Clark, S. Saubern, J. Adams, M.P. Winters, D.M.T. Chan, A. Combs, Tetrahedron Lett. 39 (1998) 2941–2944.
[28] D.A. Evans, J.L. Katz, T.R. West, Tetrahedron Lett. 39 (1998) 2937–2940.
[29] J.P. Collman, M. Zhong, Org. Lett. 2 (2000) 1233–1236.
[30] J.C. Antilla, S.L. Buchwald, Org. Lett. 3 (2001) 2077–2079.
[31] P.Y.S. Lam, G. Vincent, C.G. Clark, S. Deudon, P.K. Jadhav, Tetrahedron Lett. 42 (2001) 3415–3418.
[32] J.P. Finet, A.Y. Fedorov, S. Combes, G. Boyer, Curr. Org. Chem. 6 (2002) 597–626.
[33] T.D. Quach, R.A. Batey, Org. Lett. 5 (2003) 4397–4400.
[34] J.B. Lan, G.L. Zhang, J.S. You, L. Chen, M. Yan, R.G. Xie, Synlett (2004) 1095–1097.
[35] C. Moessner, C. Bolm, Org. Lett. 7 (2005) 2667–2669.
[36] B. Sreedhar, G.T. Venkanna, K.B.S. Kumar, V. Balasubrahmanyam, Synthesis (2008) 795–799.
[37] V. Collot, P.R. Bovyb, S. Raulta, Tetrahedron Lett. 41 (2000) 9053–9057.
[38] A.P. Combs, S. Saubern, M. Rafalski, P.Y.S. Lam, Tetrahedron Lett. 40 (1999) 1623–1626.
[39] S. Hayat, Atta-Ur-Rahman, M.I. Choudhary, Khan K.M., W. Schumann, E. Baye, Tetrahedron 57 (2001), 9951-9951.
[40] A.P. Combs, S. Tadesse, M. Rafalski, T.S. Haque, P.Y.S. Lam, J. Comb. Chem. 4 (2002) 179–182.
[41] G.C.H. Chiang, T. Olsson, Org. Lett. 6 (2004) 3079–3082.
[42] M.L. Kantam, G.T. Venkanna, C. Sridhar, B. Sreedhar, B.M. Choudary, J. Org. Chem. 71 (2006) 9522–9524.
[43] B. Kaboudin, Y. Abedi, T. Yokomatsu, Eur. J. Org. Chem. (2011) 6656–6662.
[44] J.X. Qiao, P.Y.S. Lam, Synthesis (2011) 829–856.
[45] D.S. Raghuvanshi, A.K. Gupta, K.N. Singh, Org. Lett. 14 (2012) 4326–4329.
[46] H. Pellissier, Tetrahedron 63 (2007) 1297–1330.
[47] X.Q. Zhang, Y.Y. Li, Z.R. Dong, W.Y. Shen, Z.B. Cheng, J.X. Gao, J. Mol. Catal. A: Chem. 307 (2009) 149–153.
[48] M.M. Mellah, B. Ansel, F. Patureau, A. Voituriez, E. Schulz, J. Mol. Catal. A: Chem. 272 (2007) 20–25.
[49] A. Zulauf, M. Mellah, E. Schulz, J. Org. Chem. 74 (2009) 2242–2245.
[50] G. Kubas, J. Inorg. Synth 19 (1979) 93.
[51] R.L. Dutta, A. Syamal, Elements of Magnetochemistry, Affiliated East-West Press Pvt. Ltd., New Delhi, 1993.
[52] G.M. Sheldrick, Acta Crystallogr. Sect. A 46 (1990) 467.
[53] G.M. Sheldrick, SHELXL-97, Program for Crystal Structure Refinement, University of Gottingen, Germany, 1997.
[54] I.J. Bruno, J.C. Cole, P.R. Edgington, M. Kessler, C.F. Macrae, P. McCabe, J. Pearson, R. Taylor, Acta Crystallogr. Sect. B 58 (2002) 389.
[55] L.J. Farrugia, J. Appl. Crystallogr. 30 (1997) 565–566.
[56] W.J. Geary, Coord. Chem. Rev. 7 (1971) 81–122.
[57] A.A. El-Sherif, Inorg. Chim. Acta 362 (2009) 4991–5000.
[58] T. Ghosh, B. Mondal, T. Ghosh, M. Sutradhar, G. Mukherjee, M.G.B. Drew, Inorg. Chim. Acta 360 (2007) 1753–1761.
[59] N.K. Ngan, K.M. Lo, C.S.R. Wong, Polyhedron 30 (2011) 2922–2932.
[60] V.P. Singh, D.P. Singh, Macromol. Res. 21 (2013) 757–766.
[61] M.R. Maurya, S. Agrawal, C. Bader, D. Rehder, Eur. J. Inorg. Chem. (2005) 147–157.
[62] M.R. Maurya, S. Khurana, C. Schulzke, D. Rehder, Eur. J. Inorg. Chem. (2001) 779–788.
[63] A.B.P. Lever, Inorganic Electronic Spectroscopy, second ed., Elsevier, Amsterdam, 1984.
[64] F.A. Cotton, G. Wilkinson, C.A. Murillo, M. Bachmann, Advanced Inorganic Chemistry, sixth ed., Wiley, New York, 2003.
[65] O.I. Singh, M. Damayanti, N.R. Singh, R.K.H. Singh, M. Mohapatra, R.M. Kadam, Polyhedron 24 (2005) 909–916.
[66] P. Bindu, M.R.P. Kurup, T.R. Satyakeerty, Polyhedron 18 (1999) 321–331.
[67] S. Thakurta, P. Roy, G. Rosair, C.J.G. Garcia, E. Garribba, S. Mitra, Polyhedron 28 (2009) 695–702.
[68] P. Parpot, A.P. Bettencourt, G. Chamoulaud, K.B. Kokoh, E.M. Belgsir, Electrochim. Acta 49 (2004) 397–403.
[69] V.P. Singh, S. Singh, Acta Crystallogr. Sect. E 66 (2010) o1172.
[70] G.J. Xiao, C. Wei, Acta Crystallogr. Sect. E 65 (2009) o585.
[71] J.P. Conde, M.R.J. Elsegood, K.S. Ryder, Acta Crystallogr. Sect. C 60 (2004) o166.
[72] K.B. Gudasi, R.V. Shenoy, R.S. Vadavi, S.A. Patil, M. Nethaji, J. Mol. Struct. 788 (2006) 22–29.
[73] W.X. Ni, M. Li, S.Z. Zhan, J.Z. Hou, D. Li, Inorg. Chem. 48 (2009) 1433–1441.
[74] N.K. Singh, M.K. Bharty, S.K. Kushawaha, R. Dulare, R.J. Butcher, Transit. Met. Chem. 35 (2010) 337–344.
[75] H. Tsubaki, S. Tohyama, K. Koike, H. Saitoh, O. Ishitani, Dalton Trans. (2005) 385–395.